Applied and Environmental Microbiology, Dec. 2009, p. 7674–7681 Vol. 75, No. 24
0099-2240/09/$12.00 doi:10.1128/AEM.01142-09

Analyses of Current-Generating Mechanisms of *Shewanella loihica* PV-4 and *Shewanella oneidensis* MR-1 in Microbial Fuel Cells▽†

Gregory J. Newton,[1] Shigeki Mori,[1] Ryuhei Nakamura,[2] Kazuhito Hashimoto,[1,2]* and Kazuya Watanabe[1,3]*

Hashimoto Light Energy Conversion Project, ERATO/JST, Komaba Open Laboratory, The University of Tokyo, 4-6-1 Komaba, Meguro-ku, Tokyo 153-8904, Japan[1]; Department of Applied Chemistry, The University of Tokyo, 7-3-1 Hongo, Bunkyo-ku, Tokyo 113-8656, Japan[2]; and Research Center for Advanced Science and Technology, The University of Tokyo, 4-6-1 Komaba, Tokyo 153-8904, Japan[3]

Received 18 May 2009/Accepted 6 October 2009

Although members of the genus *Shewanella* have common features (e.g., the presence of decaheme *c*-type cytochromes [*c*-cyts]), they are widely variable in genetic and physiological features. The present study compared the current-generating ability of *S. loihica* PV-4 in microbial fuel cells (MFCs) with that of well-characterized *S. oneidensis* MR-1 and examined the roles of *c*-cyts in extracellular electron transfer. We found that strains PV-4 and MR-1 exhibited notable differences in current-generating mechanisms. While the MR-1 MFCs maintained a constant current density over time, the PV-4 MFCs continued to increase in current density and finally surpassed the MR-1 MFCs. Coulombic efficiencies reached 26% in the PV-4 MFC but 16% in the MR-1 MFCs. Although both organisms produced quinone-like compounds, anode exchange experiments showed that anode-attached cells of PV-4 produced sevenfold more current than planktonic cells in the same chamber, while planktonic cells of MR-1 produced twice the current of the anode-attached cells. Examination of the genome sequence indicated that PV-4 has more *c*-cyt genes in the metal reductase-containing locus than MR-1. Mutational analysis revealed that PV-4 relied predominantly on a homologue of the decaheme *c*-cyt MtrC in MR-1 for current generation, even though it also possesses two homologues of the decaheme *c*-cyt OmcA in MR-1. These results suggest that current generation in a PV-4 MFC is in large part accomplished by anode-attached cells, in which the MtrC homologue constitutes the main path of electrons toward the anode.

Some species of dissimilatory metal-reducing bacteria (DMRB) are able to reduce solid metal oxides as terminal electron acceptors and generate currents in microbial fuel cells (MFCs) (2, 11, 14, 30, 46). Although mixed cultures are often used in MFC experiments (13), studies seeking a mechanistic understanding of electron transfer to electrode surfaces typically target pure cultures of such DMRB, due to the complexity in microbial communities. Presently, two model DMRB, *Shewanella oneidensis* MR-1 and *Geobacter sulfurreducens* PCA (2, 3, 12, 18, 31), are used in most investigations.

S. oneidensis MR-1 is a metabolically diverse DMRB that has been studied extensively for its potential use in bioremediation applications. For this reason, MR-1 was the first *Shewanella* species to have its genome completely sequenced and annotated (10). In addition, since the first report in 1999 when this microorganism was shown to have the ability to transfer electrons to the electrode without an exogenously added mediator (14), it has also become one of the model organisms for the study of electron transfer mechanisms in MFCs.

Although the molecular mechanisms for extracellular electron transfer have not yet been elucidated fully, *c*-type cytochromes (*c*-cyts) appear to be the key cellular components involved in this process (38). In *S. oneidensis* MR-1, OmcA and MtrC are outer membrane (OM), decaheme *c*-cyts that are considered to be involved in the direct (directly attached) electron transfer to solid metal oxides and anodes of MFCs (9, 20, 22, 23, 47). Several pieces of evidence suggest that OmcA and MtrC form a complex and act in a cooperative manner (33, 37, 42), and these results correlate with the fact that the genes encoding these proteins constitute an operon-like cluster in the chromosome (1). It has also been shown that MtrC and OmcA have overlapping functions as terminal reductases of metal oxides (25, 38). OmcA and MtrC are also present on the surface of nanowires and may be involved in the long-range transfer of electrons (8). In addition to direct electron transfer, MR-1 has the ability to produce water-soluble electron-shuttle compounds (quinones and flavins) that are involved in the mediated electron transfer from cells to distant solid electron acceptors (metal oxides or MFC anodes) (21, 27, 44).

Recently, the genome sequences of nearly 20 *Shewanella* strains have been completed and annotated, opening the door to study the diversity of their extracellular electron transfer mechanisms. A comparison of their genomes has shown that although they have some consensus OM *c*-cyt genes, variations exist in the number and order of these genes in their metal reductase-containing loci (6). One such species is *S. loihica* strain PV-4, which was recently isolated from an iron-rich microbial mat near a deep-sea hydrothermal vent located on the Loihi Seamount in Hawaii (7, 32). The phenotypic and phylogenetic characteristics of PV-4 were determined, with a

* Corresponding author. Mailing address: 305 Komaba Open Laboratory, The University of Tokyo, 4-6-1 Komaba, Meguro-ku, Tokyo 153-8904, Japan. Phone: 81 3 5452 5749. Fax: 81 3 5452 5749. E-mail for Kazuhito Hashimoto: hashimoto@light.t.u-tokyo.ac.jp. E-mail for Kazuya Watanabe: watanabe@light.t.u-tokyo.ac.jp.

† Supplemental material for this article may be found at http://aem.asm.org/.

▽ Published ahead of print on 16 October 2009.

TABLE 1. Bacterial strains and plasmids used in this study

Strain or plasmid	Relevant characteristic	Reference and/or source
Escherichia coli strains		
JM109 λ*pir*	Host for cloning pSMV10; *endA gyrA96 hsdR17*($r_K^-m_K^+$) *recA1 relA1 supE44 thi-1* del(*lac-proAB*) [F′ *traD36 proAB lacI*^{q}*Z*delM15] λ*pir*$^+$	29
WM6026	Donor strain for conjugation; *lacI*^{q} *rrnB3* DE*lacZ4787 hsdR514* DE(*araBAD*)*567 E*(*rhaBAD*)*568 rph-1 att-lambda*::*pAE12*-del(*oriR6K-cat*::*frt5*) DE(*endA*)::*frt uidA*(del*MluI*)::*pir*(wt) *attHK*::pJK1006-*del1/2* (del*oriR6K-cat*::*frt5* del*trfA*::*frt*)	William Metcalf, University of Illinois
DH5α	Host for cloning; F$^-$, ϕ80d*lacZ*ΔM15, Δ(*lacZYA-argF*)*U169 deoR recA1 endA1 hsdR17*($r_K^-m_K^+$) *phoA supE44* λ$^-$ *thi-1 gyrA96 relA1*	Takara Bio, Inc., Japan
S. oneidensis strains		
MR-1	Wild type	ATCC (44)
ΔmtrC mutant	*mtrC* (SO_1778) disrupted	This study
S. loihica strains		
PV-4	Wild type	ATCC (8)
Δ2522 mutant	*shew2522* disrupted	This study
Δ2523 mutant	*shew2523* disrupted	This study
Δ2525 mutant	*shew2525* disrupted	This study
Δ2522 Δ2524 mutant	*shew2522* and *shew2524* disrupted	This study
Δ2525-p2525 mutant	Δ2525 mutant harboring p2525	This study
Δ2525-pmtrC mutant	Δ2525 mutant harboring pmtrC	This study
Plasmids/vectors		
pSMV10	9.1-kb mobilizable suicide vector; *oriR6K mobRP4 sacB* Km^r Gm^r	Chad Saltikov, California Institute of Technology
pBBR1-MCS5	5.1-kb broad-host-range plasmid; Gm^r *lacZ*	17
pSMV-2522	1.5-kb fusion PCR fragment containing Δ2522 cloned into the SpeI site of pSMV10	This study
pSMV-2523	1.5-kb fusion PCR fragment containing Δ2523 cloned into the SpeI site of pSMV10	This study
pSMV-2524	1.5-kb fusion PCR fragment containing Δ2524 cloned into the SpeI site of pSMV10	This study
pSMV-2525	1.5-kb fusion PCR fragment containing Δ2525 cloned into the SpeI site of pSMV10	This study
p2525	*shew2525* PCR fragment including the promoter region cloned into the EcoRI/XbaI sites of pBBR1-MCS5	This study
pmtrC	*mtrC* PCR fragment cloned into the EcoRI/XbaI sites of pBBR1-MCS5	This study

subsequent study focusing on the metal reduction and iron biomineralization capabilities of this bacterium (32). Initial experiments performed in our laboratory revealed that PV-4 developed a *c*-cyt-dependent deep red color that was much more striking than that of strain MR-1 when grown anaerobically with iron oxide as the terminal electron acceptor (26). This allowed us to assume that PV-4 could have a high extracellular electron transfer ability. Accordingly, the present study evaluated the current-producing ability of strain PV-4 in MFCs and examined the roles of some *c*-cyts in extracellular electron transfer. Special attention was paid to the comparison of PV-4 with MR-1 to reveal differences in mechanisms for extracellular electron transfer. We report herein differences between these strains in the roles of OM *c*-cyts for extracellular electron transfer, the behaviors and metabolic patterns of MFC, and the resultant MFC performances.

MATERIALS AND METHODS

Bacterial strains, plasmids, and growth conditions. The bacterial strains and plasmids used in this study are listed in Table 1. *Escherichia coli* strains were routinely cultured in Luria-Bertani (LB) medium supplemented with appropriate antibiotics at 37°C. The *E. coli* mating strain (WM6026) required a medium supplemented with 2,6-diaminopimelic acid (DAP) at 100 μg ml^{-1} for growth. *Shewanella* strains were cultured in LB medium at 30°C, and a defined medium (named DM in this study) previously reported by Roh et al. (32) was used in MFC experiments and growth tests. Agar plates contained 1.5% Bacto agar (Difco). Lactate was used as the growth substrate in the DM.

Gene disruption and complementation. The in-frame disruption of genes in strains PV-4 and MR-1 was performed using suicide vector pSMV10 and a two-step homologous recombination method as described by Saltikov and Newman (35). Briefly, a 1.5-kb fusion product, consisting of an upstream sequence of a target gene (approximately 700 bp), replacement sequence (75 bp), and downstream sequence (approximately 700 bp), was constructed by PCR and in vitro extension using primers listed in Table S1 in the supplemental material. This fusion product was ligated to pSMV10 at the SpeI site, and *E. coli* JM109 λ*pir* was transformed with the resultant plasmid. After checking the construct, it was used to transform *E. coli* WM6026 (a *dap* auxotroph) and mated with *S. loihica* PV-4 for 5 to 8 h on LB plus DAP at 30°C. Transconjugants were selected on plates with LB plus kanamycin (60 μg ml^{-1}), and the integration site was confirmed by PCR. Next, kanamycin-sensitive clones were selected by comparing colonies grown on agar plates containing LB plus 10% sucrose and those transferred onto LB-plus-kanamycin plates. To confirm the disruption of a target gene, colonies with a kanamycin-sensitive phenotype were checked by PCR.

The broad-host-range plasmid pBBR1-MCS5 (16) was used to generate a complementation vector, to which a DNA fragment amplified from the genome of MR-1 or PV-4 using primers listed in Table S1 in the supplemental material was ligated. The complementation vectors were introduced into *Shewanella* mutant strains with the assistance of *E. coli* WM6026, and transconjugants were selected on LB agar plates containing kanamycin.

Operation and analyses of MFC. Current production was evaluated using a single-chamber MFC (similar to those used in a previous study [15]) equipped with a graphite-felt anode (5 by 10 cm in size [Sogoh Carbon]) and a platinum catalyst-doped air cathode (approximately 20 cm^2 and 0.7 mg platinum cm^{-1}) that was made as described by Cheng et al. (4). The anode chamber contained 400 ml of the DM supplemented with 10 mM lactate, and the reactor was assembled in an anaerobic chamber (Takasugi) filled with nitrogen gas treated with a reduced-copper column to remove oxygen. The MFC was inoculated with 4 ml of a stationary-phase culture grown aerobically in the DM supplemented with 10 mM lactate. The MFCs were operated at 25°C throughout the course of the experiment. The anode medium was agitated using a magnetic stirrer at approximately 100 rpm. The anode and cathode were connected with an electric wire and an external resistor (100 Ω), and the voltage across the resistor was

measured using a voltage data logger (NR-110 data acquisition system [Keyence]). When lactate was exhausted from the MFC, a 1 M stock solution of lactate was injected into the reactor to give a final concentration of 10 mM. Current (I, in amperes) was calculated using the equation $I = V/R$ (where V is the cell voltage in volts and R is the resistance in ohms), while current density ($\mu A\ cm^{-2}$) was calculated using an anode projection area of 50 cm^2. Coulombic efficiency (ε_c) was calculated by dividing the total coulombs transferred to the anode by the theoretical maximum coulombs (the total coulombs produced by complete substrate oxidation to carbon dioxide), as described elsewhere (19). Reproducibility was checked in at least three independent operations. A polarization curve was made using a potentiostat (HSV-100; Hokuto Denko), from which open-circuit voltage (V_{oc}), short-circuit current density (I_{sc}), and maximum power density (P_{max}) were obtained as described elsewhere (19).

Metabolite detection. Lactate, acetate, and some other organic acids in the MFC supernatant were measured using high-performance liquid chromatography (HPLC; Agilent), after the cells were removed by filtration through a cassette membrane (0.22 μm in pore size, DISMIC-13HP; Advantec). For the HPLC, a Zorbax column (SB-Aq, 4.6 by 150 mm; Agilent) was used under the following conditions: mobile phase, 20 mM potassium phosphate buffer (pH 2) containing 10% acetonitrile; flow rate, 1 ml min^{-1}; injection volume, 5 μl; column temperature, 45°C; and detection, UV 210 nm. Species and concentrations of the metabolites were identified based on the retention times and peak areas of pure standard compounds, including formate (2.0 min), malate (2.2 min), lactate (2.3 min), acetate (2.5 min), citrate (2.9 min), succinate (3.2 min), maleate (3.5 min), propionate (3.7 min), and fumarate (4.4 min).

Protein content. To determine the total protein content of planktonic cells in each reactor, cells were collected from the MFC medium by centrifugation at 5,000 × *g* for 10 min and resuspended in 50 ml of phosphate-buffered saline (PBS) (137 mM NaCl, 2.7 mM KCl, 4.3 mM $Na_2HPO_4 \cdot 7H_2O$, 1.4 mM KH_2PO_4, pH 7.3). For the protein assay, 1 ml of this suspension was centrifuged at 15,000 × *g* for 5 min, and the pellet was resuspended in 150 μl of B-PER II bacterial protein extraction reagent (Pierce) to solubilize the proteins according to the manufacturer's instructions. The protein concentration was determined using the Micro BCA protein assay kit (Pierce) according to the manufacturer's instructions. To determine the protein content of cells attached onto the MFC graphite-felt anode, the anodes were placed in a 250-ml centrifuge bottle with 200 ml PBS and shaken vigorously over a 5-min period. The anodes were removed, and the cells were then pelleted by centrifugation at 5,000 × *g* for 10 min and resuspended in 50 ml of PBS. The cell detachment was confirmed by microscopy. The protein content was then determined as described above. The total protein content in an MFC was the sum of protein contents from the planktonic and anode-attached cells.

Fluorescence spectrophotometry. To prepare samples for the measurement, 5 ml of the MFC supernatants from PV-4 and MR-1 reactors that had been operated for 30 days were passed through 0.2-μm-pore-size membrane filters (Advantec). Fluorescence spectra of the filtrates were recorded using a Shimadzu FP-6600 spectrometer using a 10- by 10-mm quartz cell. The emission spectra were measured using an excitation wavelength of 350 nm, and the excitation spectra were monitored at 430 nm.

Manganese reduction. Bottles (approximately 40 ml in capacity) containing 25 ml of the DM supplemented with 10 mM lactate and 6 mM manganese(IV) oxide (MnO_2) were prepared in triplicate according to a method described elsewhere (22). They were capped with Teflon-coated butyl rubber septums, sealed with aluminum crimp seals, purged with pure nitrogen gas, and inoculated with 0.25 ml of a bacterial suspension with an optical density at 600 nm (OD_{600}) of 0.1. The bottles were incubated at 30°C with shaking (150 rpm) in the course of the experiment. At appropriate time points, the amount of Mn(IV) in each sample was quantified using a colorimetric assay with leucoberbelin blue (LBB) (17). Briefly, 0.1 ml of sample was taken from a bottle, mixed with 0.9 ml of LBB solution (0.04% [wt/vol] LBB in 0.25% [vol/vol] acetic acid), and incubated in the dark for 15 min prior to measuring the OD_{690} using a spectrophotometer (DU800; Beckman). A standard curve was generated using known concentrations of $KMnO_4$ (Wako) and used to determine the concentration of Mn(IV) in a test sample.

Iron reduction. Bottles containing 25 ml of the DM supplemented with 10 mM lactate and 10 mM iron citrate (Sigma) were prepared in duplicate and inoculated with 0.25 ml of a bacterial suspension with an OD_{600} of 0.1. The amount of Fe(II) ion produced in each bottle was quantified using a colorimetric ferrozine assay (40, 41). Briefly, a 200-μl sample was taken from the bottle, mixed with 800 μl of 0.625 N HCl, and incubated for 15 min at room temperature. This solution was then spun at 16,000 × *g* for 5 min, and 50 μl of the supernatant was mixed with 950 μl of 2 mM ferrozine solution (in 50 mM HEPES buffer, pH 7.0). After 1 min, the absorbance at 562 nm was measured. The concentration of Fe(II) in a test sample was determined using a standard curve generated using known concentrations of $FeSO_4 \cdot 7H_2O$ (Wako).

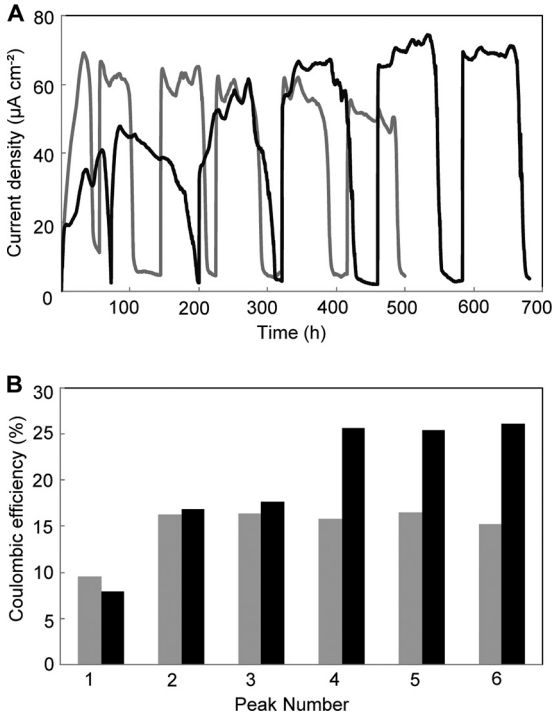

FIG. 1. A comparison of the current densities (A) and ε_c values (B) for *S. oneidensis* MR-1 (gray line, gray bars) and *S. loihica* PV-4 (black line, black bars) in single-chamber MFCs operated for approximately 30 days.

RESULTS

Comparison of MFCs harboring strains PV-4 and MR-1. We initially compared the profiles of current production in PV-4 and MR-1 MFCs (Fig. 1A). The current density for MR-1 sharply increased from the time of initial inoculation and typically reached its peak level of current density within 24 h. After the lactate in the medium was exhausted, the current density decreased to nearly 0. However, upon injection of lactate into the reactor, the resumption of current occurred rapidly, and within approximately 15 min had reached the previous peak value. MR-1 showed a very regular pattern for current production when the lactate was exhausted and replenished over five injections, with the current density remaining fairly constant at approximately 60 $\mu A\ cm^{-2}$. After the second injection of lactate, ε_c increased approximately 1.8-fold (from 9% to 16%) and remained constant at approximately 16% (15.9 ± 0.6% [mean ± standard deviation] for the last three peaks) for the remainder of the experiment (Fig. 1B).

The profile of current production for PV-4 was quite different compared to MR-1 (Fig. 1A). Initially, the current production in the PV-4 MFC increased at a level similar to that of MR-1, but at a current density of 20 $\mu A\ cm^{-2}$, the current invariably reached a minor peak that fell slightly before increasing again. The current then increased until it reached a peak current density of approximately 40 $\mu A\ cm^{-2}$, although the initial ε_c values were nearly identical (Fig. 1B). With re-

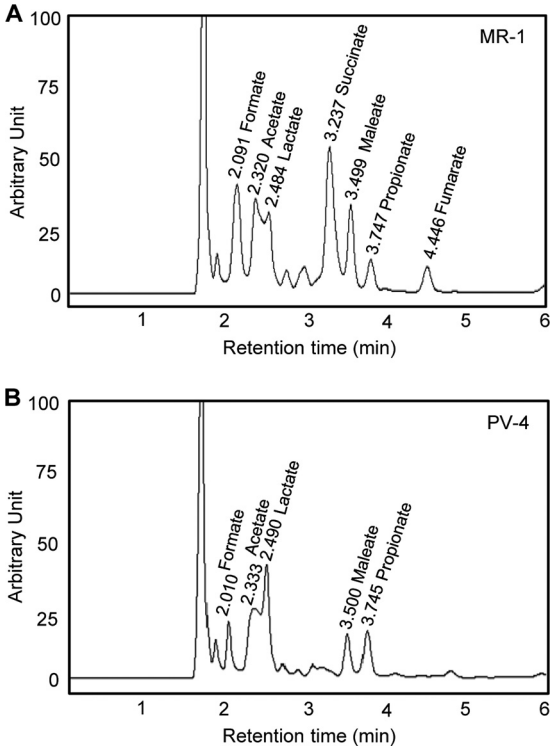

FIG. 2. HPLC patterns for the media from the MR-1 (A) and PV-4 (B) MFC reactors, showing the occurrences of organic acids. The retention times (min) and corresponding compounds are shown above the major peaks.

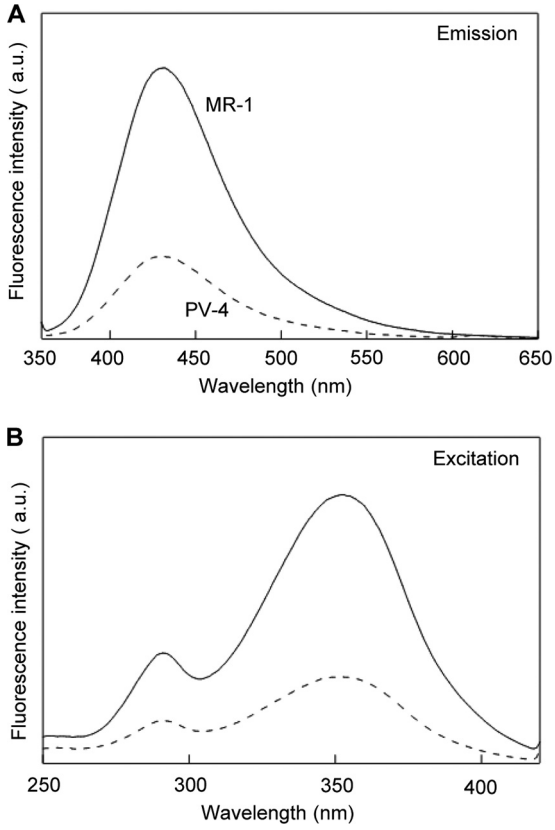

FIG. 3. Fluorescence spectra for the filtered supernatants from MFCs with strains PV-4 (dotted line) and MR-1 (solid line). (A) Emission spectra with the excitation at 350 nm. (B) Excitation spectra measured at 430 nm. a.u., arbitrary unit.

peated injections of lactate, both the current density and ε_c increased and reached 74 μA cm^{-2} and 26% (25.8% $\pm$ 0.3% for the last three peaks), respectively, after the fourth injection of lactate (at approximately hour 500). This ε_c value was significantly higher than that of MR-1. After the fifth addition of lactate, V_{oc}, I_{sc}, and P_{max} for the PV-4 MFC were determined to be 0.62 V, 0.19 mA cm^{-2}, and 44 μW cm^{-2}, respectively, while those for the MR-1 MFC were 0.58 V, 0.15 mA cm^{-2}, and 31 μW cm^{-2}, respectively.

After the sixth addition of lactate (60 mM in total), the metabolites in the anode medium were analyzed by HPLC (Fig. 2). We found that more metabolites (organic acids) were detected in the MR-1 medium than in the PV-4 medium. Most notable was the accumulation of acetate in the MR-1 medium (21 mM), followed by succinate (17 mM), formate (16 mM), and some other compounds. In the PV-4 MFC, acetate was the most abundant metabolite and reached approximately 13 mM. We also compared the total protein content in the PV-4 and MR-1 MFCs. For PV-4, the total protein was determined to be 22.8 $\pm$ 1.7 mg (mean $\pm$ standard deviation), while MR-1 maintained a higher overall biomass, with a total protein content of 28.1 $\pm$ 2.2 mg in the MFC reactor.

It has previously been reported that MR-1 produces two types of extracellular electron shuttles (quinones [27] and flavins [21, 44]). Since they can be distinguished based on their distinct fluorescence spectra, we subjected the supernatants of the PV-4 and MR-1 reactors to spectrophotometric analyses. We found that the fluorescence spectra of these two strains were very similar (Fig. 3), indicating that they produced similar compounds in the MFC medium. In the fluorescence emission spectra of the MR-1 and PV-4 reactor supernatants (Fig. 3A), peak emission wavelengths of approximately 420 nm were detected (Fig. 3A), suggesting the presence of quinone derivatives. This was confirmed by excitation peaks of 350 nm (Fig. 3B) (5, 29). These figures also indicate that MR-1 produced more quinone derivatives than PV-4.

Anode-exchange experiment. To examine the contribution of anode-attached versus planktonic cells toward current density, the anode of an MFC operating at the steady state was transferred into a new MFC reactor (anode-MFC), while a new anode was placed in the original MFC medium (supernatant-MFC). When the anodes were taken out of the reactors, current densities of approximately 40 and 70 μA cm^{-2} were recorded for the original MR-1 and PV-4 MFCs, respectively. For each new reactor, the current density was measured for approximately 8 h after performing the exchange (Fig. 4). We found that the contributions of attached and planktonic cells toward the current density were very different between the two species. In the case of MR-1, the supernatant-MFC had a higher initial current density than in the anode-MFC, with current densities of 11 μA cm^{-2} and 5 μA cm^{-2}, respectively (Fig. 4A). In the supernatant-MFC, the current density rapidly increased and stabilized at approximately 40 μA cm^{-2}, while the current density in the anode-MFC gradually increased dur-

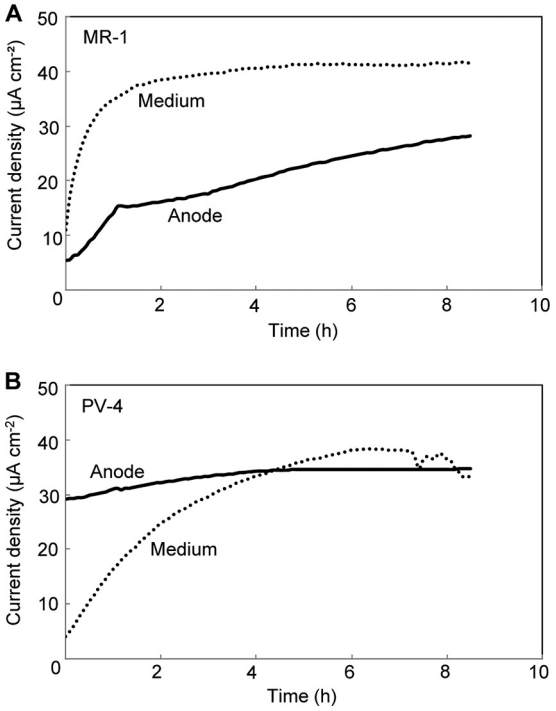

FIG. 4. Current generation in the anode exchange experiments in which the anode from a single-chamber MFC of *S. oneidensis* MR-1 (A) or *S. loihica* PV-4 (B), which had run for 30 days, was transferred into a new MFC containing fresh medium (solid line) or a new anode was placed into the original reactor (dotted line).

ing the measurement. These data indicate that planktonic cells contributed more to the current generation in the original MR-1 MFC than in anode-attached cells. In the PV-4 MFC, however, the contribution trend was reversed; namely, the anode-MFC showed an initial current density of 29 μA cm^{-2}, which was much larger than the 4 μA cm^{-2} for the supernatant-MFC (Fig. 4B). After approximately 4 h, both reactors reached the same current density of approximately 35 μA cm^{-2}.

Disruption of genes for OM *c*-cyts. PV-4 has a genomic region that corresponds to a metal-reducing *c*-cyt gene cluster found in many *Shewanella* strains (6). Figure 5 shows a comparison of the gene clusters in MR-1 and PV-4, displaying the similarities and differences in the gene organization. While the flanking *mtrDEF* and *mtrCAB* regions had corresponding homologues in PV-4 in the same position and order (coding for predicted proteins that ranged from 50.6% to 82.3% amino acid identity [Table 2]), there were two copies of genes (*shew2522* and *shew2524*) coding for predicted proteins with a high level of homology to OmcA of MR-1 (58.3% and 64.2% amino acid identity, respectively [Table 2]). These open reading frames (ORFs) flanked a predicted decaheme *c*-cyt gene (*shew2523*) that shared the closest homology to OmcA (28.7% amino acid identity), mostly in the amino terminal of the predicted protein. An NCBI BLAST search revealed that ORF2523 shares the highest degree of homology (65.4% identity) with a putative decaheme *c*-cyt (the NapC/NirT *c*-cyt family) of *Shewanella piezotolerans* WP3 (45), which, like strain PV-4, is also a deep-sea isolate.

TABLE 2. A comparison of the predicted *c*-cyt proteins from *S. loihica* PV-4 and the closest homologous proteins in *S. oneidensis* MR-1

S. loihica PV-4 ORF		*S. oneidensis* MR-1 ORF		Identity (%)
Name	Size (aa)[a]	Name	Size (aa)	
Shew_2519	322	*mtrD* (SO_1782)	306	72.7
Shew_2520	703	*mtrE* (SO_1781)	712	50.6
Shew_2521	639	*mtrF* (SO_1780)	639	62.7
Shew_2522	720	*omcA* (SO_1779)	735	58.3
Shew_2523	757	*omcA* (SO_1779)	735	28.7
Shew_2524	725	*omcA* (SO_1779)	735	64.2
Shew_2525	664	*mtrC* (SO_1778)	671	63.3
Shew_2526	332	*mtrA* (SO_1777)	333	82.3
Shew_2527	699	*mtrB* (SO_1776)	697	69.9

[a] aa, amino acids.

To determine the contribution of the predicted decaheme *c*-cyts in extracellular electron transfer, in-frame deletion mutants were made with *shew2522*, *shew2523*, and *shew2525*, along with a double mutant with *shew2522* and *shew2524* (Table 1), and current generation by these mutants was analyzed (Fig. 6). The mutants lacking the OmcA homologues (Shew_2522 and Shew_2524) and the mutant lacking *shew2523*, the unique decaheme *c*-cyt gene, generated current densities that were slightly lower than the current density produced by wild-type PV-4. In contrast, the PV-4 mutant lacking the *mtrC* homologue (carrying Δ2525) was severely impaired for current production, reaching a maximum current density of only 9.1% of that attained by the wild-type cells. This was different from the case of *mtrC* in MR-1, since the *mtrC* deletion mutant still produced over 40% of the wild-type current density. The complemented mutant (carrying Δ2525-p2525) was able to produce a current density similar to that of wild-type PV-4 (Fig. 6). Interestingly, complementation of the

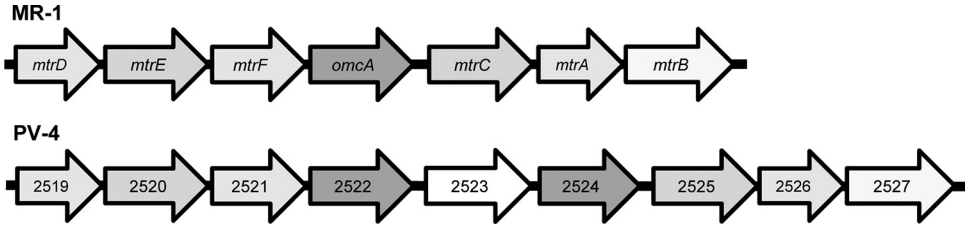

FIG. 5. Organization of the *mtrDEF-omcA-mtrCAB* *c*-cyt-rich region in strain MR-1 and a homologous region in strain PV-4. This region corresponds to the genome coordinates 1856169 to 1869171 in MR-1 (TIGR annotation) and 2982508 to 2964239 in PV-4 (DOE Joint Genome Institute annotation).

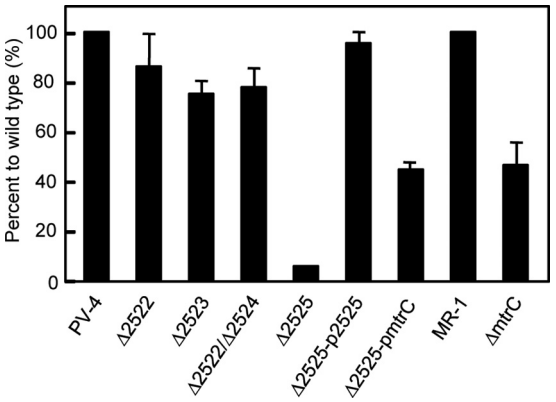

FIG. 6. Comparison of current densities in MFCs inoculated with knockout mutants versus the wild-type strain (PV-4 or MR-1).

Δ2525 mutant with the *mtrC* gene from MR-1 was also able to restore the current-producing ability, although it was only approximately one-half the wild-type PV-4 level (Fig. 6).

Metal reduction by the mutant strains. Since we found differences between MR-1 and PV-4 in the roles of OM *c*-cyts in current generation in MFCs, we thought it would also be interesting to examine their roles in iron and manganese reduction (Table 3). Iron citrate is soluble in water, and it has been suggested that it can be reduced by strain MR-1 using intercellular and extracellular reductases (34). In contrast, manganese oxide is amorphous and reduced only via extracellular electron transfer (38). We considered that it should be interesting to examine the roles of OM *c*-cyts for the reduction of iron citrate and manganese oxide.

The reduction rates of the Δ2522, Δ2522 Δ2524, and Δ2523 mutants for iron citrate and manganese oxide were not significantly different from those of the wild-type PV-4 (data not shown). However, the Δ2525 mutant was highly impaired for both electron acceptors (Table 3), confirming that Shew2525 is primarily important for extracellular electron transfer. The Δ2525 mutant retained only 34% of the wild-type PV-4's ability to reduce MnO_2. This is a much larger impairment than in the Δ*mtrC* mutant of MR-1, which was still able to reduce 78% of the MnO_2 that the wild-type MR-1 reduced in the same 48-h period. For iron-citrate reduction, a similar trend was observed, although for both MR-1 and PV-4, deletion of the *mtrC* and *shew2525* genes, respectively, more severely affected their abilities. The Δ2525 mutant had only 5% of the activity of the wild-type PV-4, while the ΔmtrC mutant retained 34% of the activity of the wild-type MR-1 (Table 3).

DISCUSSION

Our comparison of the MR-1 and PV-4 MFCs revealed several significant differences, including the current density, the time needed to establish a constant current, and ε_c. The current generation by a bacterium is dependent on its substrate oxidation rate (catabolic speed) and electron loss (between substrate oxidation and anode current). The current profiles (Fig. 1A) show that MR-1 more rapidly used up the lactate (10 mM) added as the sole energy source than PV-4 did, suggesting that the substrate oxidation rate of MR-1 was greater than that of PV-4. It is therefore likely that the higher current and power densities in the PV-4 MFC were ascribable to a loss of electrons smaller than that in MR-1 MFC. This conclusion is supported by the high ε_c values of the PV-4 MFC (Fig. 1B).

Several causes have been suggested for lowering ε_c in MFCs (18, 39); these include (i) incomplete oxidation of substrates, (ii) the presence of alternative electron acceptors, and (iii) assimilation (microbial growth and storage of energy sources). Concerning the first point, we analyzed the metabolites produced by MR-1 and PV-4 during the course of the MFC operation and found that more metabolites were detected in the supernatant of the MR-1 MFC (Fig. 2). For instance, the accumulation of acetate (21 mM) and succinate (17 mM) in the MR-1 MFC medium accounted for 23% and 33%, respectively, of the electrons liberated from the total amount of lactate supplied (60 mM). This indicates that the accumulation of these metabolites had the largest influences on ε_c and the current density in MFCs with these *Shewanella* strains. A previous MFC experiment showed that MR-1 consumed lactate with an approximate stoichiometric accumulation of acetate, and it was slowly metabolized without generating electric current (18). In contrast to that report, acetate was partially produced from lactate in our MFCs, and we considered that the accumulation of other metabolites (e.g., succinate) more seriously reduced the ε_c value. The difference is likely ascribable to the different types of MFC used in the experiments.

Second, the ε_c value is also affected by alternative electron acceptors. It is known that oxygen permeates through the air cathode (4) and serves as an electron acceptor for anode microbes (39). Taking into account the oxygen transfer rate through an air cathode with the same structure (1.4 μmol h^{-1} cm^{-2} [4]), the number of electrons needed to reduce each mole of oxygen (4 mol), and the air cathode area (20 cm^2), the oxygen-dependent electron consumption rate for the MFC used in this study was calculated to be equivalent to an electrical current of 3 mA. This value is almost equal to the current generated in the MR-1 MFC. This loss is, however, considered to have affected the MR-1 and PV-4 MFCs equally, since identical air cathodes were used. Finally, based on the protein content, assimilation of organics was estimated to have minor influences on the ε_c values for these *Shewanella* MFCs

TABLE 3. Iron-citrate and manganese-oxide reduction by *S. loihica* PV-4, *S. oneidensis* MR-1, and their derivatives

Strain	Manganese-oxide reduction		Iron-citrate reduction	
	Rate (μmol $liter^{-1}$ hr^{-1})[a]	Ratio to the wild type (%)	Rate (μmol $liter^{-1}$ hr^{-1})[a]	Ratio to the wild type (%)
S. loihica				
PV-4	100 ± 6.0	100	1,700 ± 66	100
Δ2525 mutant	34 ± 4.4	34	280 ± 4.0	17
Δ2525-p2525 mutant	74 ± 4.7	74	1,600 ± 35	99
Δ2525-pmtrC mutant	68 ± 15	68	1,500 ± 57	89
S. oneidensis				
MR-1	95 ± 4.2	100	1,500 ± 49	100
ΔmtrC mutant	78 ± 5.5	82	570 ± 5.1	37

[a] Mean ± standard deviation (n = 3).

(~10%). Altogether, it is considered that the difference in the ε_c values between strains MR-1 and PV-4 was ascribable mostly to the difference in their metabolite production.

Despite the fact that both mediated (via mediators) and direct (via OM *c*-cyts) electron transfer mechanisms are present in MR-1 and PV-4, the anode exchange experiment (Fig. 4) revealed that the current in the PV-4 MFC was attributed more to anode-attached cells than to planktonic cells and vice versa in the MR-1 MFC. The importance of planktonic cells for current generation in MFCs has previously been suggested for MR-1 (18). This study found that even for species in the same genus, *Shewanella*, the behaviors (e.g., growth as planktonic and anode-attached cells) in MFCs were largely different, which may have resulted from different extracellular electron transfer mechanisms employed by these strains. Anode-attached cells likely employ direct electron transfer mechanisms, as is the case with *Geobacter* (2), while organisms employing mediated electron transfer by producing soluble electron shuttles are able to thrive as planktonic cells in MFCs (36). The finding that the concentration of quinone derivatives in the anode medium in the PV-4 MFC was low compared to that in the MR-1 MFC (Fig. 3) may have been related to this notion.

Accordingly, we thought that it was important to investigate how the anode-attached cells of PV-4 transferred electrons to the MFC anode. In the model for the extracellular electron transfer pathways in MR-1 (38), MtrC and OmcA are considered to act as terminal reductases and have overlapping functions (23–25). Previous studies have also shown that a double-knockout mutant of *mtrC* and *omcA* still generated current at a level 15% of that of the wild type (3), suggesting the presence of alternative channels for the transfer of electrons to the anode in MR-1. It is considered that electron mediators (quinones and flavins) that bypass OM *c*-cyts can have this role (21, 27, 44). Unexpectedly, however, the single disruption of the gene for the MtrC homologue (*shew2525*) almost completely restrained the current generation by PV-4 (Fig. 6). The complementation experiment indicated that MtrC of MR-1 can assume the role of Shew2525 in PV-4 (Fig. 6), suggesting that Shew2525 is also a terminal reductase. These findings are consistent with the result that anode-attached cells of PV-4 contributed most to the current generation in MFC. Unexpectedly, however, the disruption of the genes for the OmcA homologues did not substantially affect the current generation by PV-4. This indicates that functions of the OmcA homologues in PV-4 (Shew2522 and Shew2524) are clearly different from those of OmcA in MR-1, since MtrC and OmcA are considered to have replaceable overlapping functions as terminal reductases for metal oxides (23, 35). Disruption of *shew2323* (putative OM *c*-cyt gene with unknown function) also did not largely impair extracellular electron transfer, and it would be interesting to examine the triple knockout of *shew2322*, *shew2323*, and *shew2324*. These results indicate that Shew2525 in PV-4 plays a crucial role in extracellular electron transfer and suggest that OM *c*-cyts are differently utilized in MR-1 and PV-4.

The metal reduction tests confirmed that Shew2525 was primarily important for extracellular electron transfer in PV-4 (Table 3). In these experiments, however, it was unexpected that the disruption of *shew2525* in PV-4 and *mtrC* in MR-1 more largely impaired iron-citrate reduction than manganese-oxide reduction. Although we do not have conclusive ideas regarding this point, such phenomena may occur if mediators contribute largely to manganese-oxide reduction.

In conclusion, the present study shows that even though MR-1 and PV-4 are affiliated with the same genus, *Shewanella*, and possess similar genes for metal-reducing *c*-cyts, they employ substantially different extracellular electron transfer mechanisms (e.g., mediated versus direct electron transfer, amounts of excreted mediators, and roles of OM *c*-cyts). At present, the genomes of nearly 20 strains in the genus *Shewanella* have been completed, and the diversity in the genetic organization of metal-reducing *c*-cyts among these strains has been analyzed (6). We suggest that further genetic and physiological studies of these diverse *Shewanella* strains are needed to comprehend the consensus features and diversity in the metal-reducing and current-generating mechanisms in this environmentally and biotechnologically important genus.

ACKNOWLEDGMENTS

We thank Yuri Gorby for the critical reading of the manuscript. We also thank William Metcalf for providing *E. coli* strain WM6026, Chad Saltikov for pSMV10, Liang Shi for pBBR1-MCS5, and the Japan National Institute of Genetics for *E. coli* JM109 λ*pir*.

This work was supported by the Exploratory Research for Advanced Technology (ERATO) program of the Japanese Science and Technology Agency (JST).

REFERENCES

1. **Beliaev, A. S., D. A. Saffarini, J. L. McLaughlin, and D. Hunnicutt.** 2001. MtrC, an outer membrane decahaem *c* cytochrome required for metal reduction in *Shewanella putrefaciens* MR-1. Mol. Microbiol. **39:**722–730.
2. **Bond, D. R., and D. R. Lovley.** 2003. Electricity production by *Geobacter sulfurreducens* attached to electrodes. Appl. Environ. Microbiol. **69:**1548–1555.
3. **Bretschger, O., A. Obraztsova, C. A. Sturm, I. S. Chang, Y. A. Gorby, S. B. Reed, D. E. Culley, C. L. Reardon, S. Barua, M. F. Romine, J. Zhou, A. S. Beliaev, R. Bouhenni, D. Saffarini, F. Mansfeld, B. H. Kim, J. K. Fredrickson, and K. H. Nealson.** 2007. Current production and metal oxide reduction by *Shewanella oneidensis* MR-1 wild type and mutants. Appl. Environ. Microbiol. **73:**7003–7012.
4. **Cheng, S., H. Liu, and B. E. Logan.** 2006. Increased power generation in a continuous flow MFC with advective flow through the porous anode and reduced electrode spacing. Environ. Sci. Technol. **40:**2426–2432.
5. **Del Vecchio, R., and N. V. Blough.** 2004. On the origin of the optical properties of humic substances. Environ. Sci. Technol. **38:**3885–3891.
6. **Fredrickson, J. K., M. F. Romine, A. S. Beliaev, J. M. Auchtung, M. E. Driscoll, T. S. Gardner, K. H. Nealson, A. L. Osterman, G. Pinchuk, J. L. Reed, D. A. Rodionov, J. L. Rodrigues, D. A. Saffarini, M. H. Serres, A. M. Spormann, I. B. Zhulin, and J. M. Tiedje.** 2008. Towards environmental systems biology of *Shewanella*. Nat. Rev. Microbiol. **6:**592–603.
7. **Gao, H., A. Obraztova, N. Stewart, R. Popa, J. K. Fredrickson, J. M. Tiedje, K. H. Nealson, and J. Zhou.** 2006. *Shewanella loihica* sp. nov., isolated from iron-rich microbial mats in the Pacific Ocean. Int. J. Syst. Evol. Microbiol. **56:**1911–1916.
8. **Gorby, Y. A., S. Yanina, J. S. McLean, K. M. Rosso, D. Moyles, A. Dohnalkova, T. J. Beveridge, I. S. Chang, B. H. Kim, K. S. Kim, D. E. Culley, S. B. Reed, M. F. Romine, D. A. Saffarini, E. A. Hill, L. Shi, D. A. Elias, D. W. Kennedy, G. Pinchuk, K. Watanabe, S. Ishii, B. Logan, K. H. Nealson, and J. K. Fredrickson.** 2006. Electrically conductive bacterial nanowires produced by *Shewanella oneidensis* strain MR-1 and other microorganisms. Proc. Natl. Acad. Sci. USA **103:**11358–11363.
9. **Hartshorne, R. S., B. N. Jepson, T. A. Clarke, S. J. Field, J. Fredrickson, J. Zachara, L. Shi, J. N. Butt, and D. J. Richardson.** 2007. Characterization of *Shewanella oneidensis* MtrC: a cell-surface decaheme cytochrome involved in respiratory electron transport to extracellular electron acceptors. J. Biol. Inorg. Chem. **12:**1083–1094.
10. **Heidelberg, J. F., I. T. Paulsen, K. E. Nelson, E. J. Gaidos, W. C. Nelson, T. D. Read, J. A. Eisen, R. Seshadri, N. Ward, B. Methe, R. A. Clayton, T. Meyer, A. Tsapin, J. Scott, M. Beanan, L. Brinkac, S. Daugherty, R. T. DeBoy, R. J. Dodson, A. S. Durkin, D. H. Haft, J. F. Kolonay, R. Madupu, J. D. Peterson, L. A. Umayam, O. White, A. M. Wolf, J. Vamathevan, J. Weidman, M. Impraim, K. Lee, K. Berry, C. Lee, J. Mueller, H. Khouri, J.**

Gill, T. R. Utterback, L. A. McDonald, T. V. Feldblyum, H. O. Smith, J. C. Venter, K. H. Nealson, and C. M. Fraser. 2002. Genome sequence of the dissimilatory metal ion-reducing bacterium *Shewanella oneidensis*. Nat. Biotechnol. **20:**1118–1123.

11. **Holmes, D. E., D. R. Bond, and D. R. Lovley.** 2004. Electron transfer by *Desulfobulbus propionicus* to Fe(III) and graphite electrodes. Appl. Environ. Microbiol. **70:**1234–1237.
12. **Holmes, D. E., S. K. Chaudhuri, K. P. Nevin, T. Mehta, B. A. Methe, A. Liu, J. E. Ward, T. L. Woodard, J. Webster, and D. R. Lovley.** 2006. Microarray and genetic analysis of electron transfer to electrodes in *Geobacter sulfurreducens*. Environ. Microbiol. **8:**1805–1815.
13. **Ishii, S., T. Shimoyama, Y. Hotta, and K. Watanabe.** 2008. Characterization of a filamentous biofilm community established in a cellulose-fed microbial fuel cell. BMC Microbiol. **8:**6.
14. **Kim, B. H., H. J. Kim, M. S. Moon, and D. H. Park.** 1999. Direct electrode reaction of Fe(III)-reducing bacterium *Shewanella putrefaciens*. J. Microbiol. Biotechnol. **9:**127–131.
15. **Kodama, Y., and K. Watanabe.** 2008. An electricity-generating prosthecate bacterium strain Mfc52 isolated from a microbial fuel cell. FEMS Microbiol. Lett. **288:**55–61.
16. **Kovach, M. E., P. H. Elzer, D. S. Hill, G. T. Robertson, M. A. Farris, R. M. Roop II, and K. M. Peterson.** 1995. Four new derivatives of the broad-host-range cloning vector pBBR1MCS, carrying different antibiotic-resistance cassettes. Gene **166:**175–176.
17. **Krumbein, W. E., and H. J. Altmann.** 1973. A new method for the detection and enumeration of manganese oxidizing and reducing microorganisms. Helgolander Wiss. Meeresunters. **25:**347–356.
18. **Lanthier, M., K. B. Gregory, and D. R. Lovley.** 2008. Growth with high planktonic biomass in *Shewanella oneidensis* fuel cells. FEMS Microbiol. Lett. **278:**29–35.
19. **Logan, B. E., B. Hamelers, R. Rozendal, U. Schroder, J. Keller, S. Freguia, P. Aelterman, W. Verstraete, and K. Rabaey.** 2006. Microbial fuel cells: methodology and technology. Environ. Sci. Technol. **40:**5181–5192.
20. **Lower, B. H., L. Shi, R. Yongsunthon, T. C. Droubay, D. E. McCready, and S. K. Lower.** 2007. Specific bonds between an iron oxide surface and outer membrane cytochromes MtrC and OmcA from *Shewanella oneidensis* MR-1. J. Bacteriol. **189:**4944–4952.
21. **Marsili, E., D. B. Baron, I. D. Shikhare, D. Coursolle, J. A. Gralnick, and D. R. Bond.** 2008. *Shewanella* secretes flavins that mediate extracellular electron transfer. Proc. Natl. Acad. Sci. USA **105:**3968–3973.
22. **Murray, J. W.** 1974. The surface chemistry of hydrous manganese dioxide. J. Colloid Interface Sci. **46:**357–371.
23. **Myers, C. R., and J. M. Myers.** 2003. Cell surface exposure of the outer membrane cytochromes of *Shewanella oneidensis* MR-1. Lett. Appl. Microbiol. **37:**254–258.
24. **Myers, J. M., and C. R. Myers.** 2001. Role for outer membrane cytochromes OmcA and OmcB of *Shewanella putrefaciens* MR-1 in reduction of manganese dioxide. Appl. Environ. Microbiol. **67:**260–269.
25. **Myers, J. M., and C. R. Myers.** 2003. Overlapping role of the outer membrane cytochromes of *Shewanella oneidensis* MR-1 in the reduction of manganese(IV) oxide. Lett. Appl. Microbiol. **37:**21–25.
26. **Nakamura, R., K. Ishii, and K. Hashimoto.** 2009. Electronic absorption spectra and redox properties of C type cytochromes in living microbes. Angew. Chem. Int. Ed. Engl. **48:**1606–1608.
27. **Newman, D. K., and R. Kolter.** 2000. A role for excreted quinones in extracellular electron transfer. Nature **405:**94–97.
28. **Penfold, R. J., and J. M. Pemberton.** 1992. An improved suicide vector for construction of chromosomal insertion mutations in bacteria. Gene **118:**145–146.
29. **Perez-Ruiz, T., C. Martinez-Lozano, M. A. Garcia, and J. Martin.** 2007. High-performance liquid chromatography: photochemical reduction in aerobic conditions for determination of K vitamins using fluorescence detection. J. Chromatogr. A **1141:**67–72.
30. **Pham, C. A., S. J. Jung, N. T. Phung, J. Lee, I. S. Chang, B. H. Kim, H. Yi, and J. Chun.** 2003. A novel electrochemically active and Fe(III)-reducing bacterium phylogenetically related to *Aeromonas hydrophila*, isolated from a microbial fuel cell. FEMS Microbiol. Lett. **223:**129–134.
31. **Reguera, G., K. P. Nevin, J. S. Nicoll, S. F. Covalla, T. L. Woodard, and D. R. Lovley.** 2006. Biofilm and nanowire production leads to increased current in *Geobacter sulfurreducens* fuel cells. Appl. Environ. Microbiol. **72:**7345–7348.
32. **Roh, Y., H. Gao, H. Vali, D. W. Kennedy, Z. K. Yang, W. Gao, A. C. Dohnalkova, R. D. Stapleton, J. W. Moon, T. J. Phelps, J. K. Fredrickson, and J. Zhou.** 2006. Metal reduction and iron biomineralization by a psychrotolerant Fe(III)-reducing bacterium, *Shewanella* sp. strain PV-4. Appl. Environ. Microbiol. **72:**3236–3244.
33. **Ross, D. E., S. S. Ruebush, S. L. Brantley, R. S. Hartshorne, T. A. Clarke, D. J. Richardson, and M. Tien.** 2007. Characterization of protein-protein interactions involved in iron reduction by *Shewanella oneidensis* MR-1. Appl. Environ. Microbiol. **73:**5797–5808.
34. **Ross, D. E., S. L. Brantley, and M. Tien.** 2009. Kinetic characterization of OmcA and MtrC, terminal reductases involved in respiratory electron transfer for dissimilatory iron reduction in *Shewanella oneidensis* MR-1. Appl. Environ. Microbiol. **75:**5218–5226.
35. **Saltikov, C. W., and D. K. Newman.** 2003. Genetic identification of a respiratory arsenate reductase. Proc. Natl. Acad. Sci. USA **100:**10983–10988.
36. **Schröder, U.** 2007. Anodic electron transfer mechanisms in microbial fuel cells and their energy efficiency. Phys. Chem. Chem. Phys. **9:**2619–2629.
37. **Shi, L., B. Chen, Z. Wang, D. A. Elias, M. U. Mayer, Y. A. Gorby, S. Ni, B. H. Lower, D. W. Kennedy, D. S. Wunschel, H. M. Mottaz, M. J. Marshall, E. A. Hill, A. S. Beliaev, J. M. Zachara, J. K. Fredrickson, and T. C. Squier.** 2006. Isolation of a high-affinity functional protein complex between OmcA and MtrC: two outer membrane decaheme *c*-type cytochromes of Shewanella oneidensis MR-1. J. Bacteriol. **188:**4705–4714.
38. **Shi, L., T. C. Squier, J. M. Zachara, and J. K. Fredrickson.** 2007. Respiration of metal (hydr)oxides by *Shewanella* and *Geobacter*: a key role for multihaem *c*-type cytochromes. Mol. Microbiol. **65:**12–20.
39. **Shimoyama, T., S. Komukai, A. Yamazawa, Y. Ueno, B. E. Logan, and K. Watanabe.** 2008. Electricity generation from model organic wastewater in a cassette-electrode microbial fuel cell. Appl. Microbiol. Biotechnol. **79:**325–330.
40. **Sørensen, J.** 1982. Reduction of ferric iron in anaerobic, marine sediment and interaction with reduction of nitrate and sulfate. Appl. Environ. Microbiol. **43:**319–324.
41. **Stookey, L. L.** 1970. Ferrozine–a new spectrophotomeric reagent for iron. Anal. Chem. **42:**779–781.
42. **Tang, X., W. Yi, G. R. Munske, D. P. Adhikari, N. L. Zakharova, and J. E. Bruce.** 2007. Profiling the membrane proteome of *Shewanella oneidensis* MR-1 with new affinity labeling probes. J. Proteome Res. **6:**724–734.
43. **Venkateswaran, K., D. P. Moser, M. E. Dollhopf, D. P. Lies, D. A. Saffarini, B. J. MacGregor, D. B. Ringelberg, D. C. White, M. Nishijima, H. Sano, J. Burghardt, E. Stackebrandt, and K. H. Nealson.** 1999. Polyphasic taxonomy of the genus *Shewanella* and description of *Shewanella oneidensis* sp. nov. Int. J. Syst. Bacteriol. **49:**705–724.
44. **von Canstein, H., J. Ogawa, S. Shimizu, and J. R. Lloyd.** 2008. Secretion of flavins by *Shewanella* species and their role in extracellular electron transfer. Appl. Environ. Microbiol. **74:**615–623.
45. **Wang, F., J. Wang, H. Jian, B. Zhang, S. Li, X. Zeng, L. Gao, D. H. Bartlett, J. Yu, S. Hu, and X. Xiao.** 2008. Environmental adaptation: genomic analysis of the piezotolerant and psychrotolerant deep-sea iron reducing bacterium *Shewanella piezotolerans* WP3. PLoS ONE **3:**e1937.
46. **Watanabe, K.** 2008. Recent developments in microbial fuel cell technologies for sustainable bioenergy. J. Biosci. Bioeng. **106:**528–536.
47. **Xiong, Y., L. Shi, B. Chen, M. U. Mayer, B. H. Lower, Y. Londer, S. Bose, M. F. Hochella, J. K. Fredrickson, and T. C. Squier.** 2006. High-affinity binding and direct electron transfer to solid metals by the *Shewanella oneidensis* MR-1 outer membrane c-type cytochrome OmcA. J. Am. Chem. Soc. **128:**13978–13979.